ANALYTICAL SCIENCES DECEMBER 2020, VOL. 36

Screening of Urinary Renal Cancer Metabolic Biomarkers with Gold Nanoparticles-assisted Laser Desorption/Ionization Mass Spectrometry

Adrian Arendowski,*† Krzysztof Ossoliński, Joanna Nizioł,* and Tomasz Ruman***

**Faculty of Chemistry, Rzeszów University of Technology, 6 Powstańców Warszawy Ave, 35-959 Rzeszów, Poland*

***Department of Urology, John Paul II District Hospital, Grunwaldzka 4 St, 36-100 Kolbuszowa, Poland*

Renal cell carcinoma is a very aggressive and often fatal disease for which there are no specific biomarkers found to date. The purpose of this work was to find features that differentiate urine metabolic profiles of healthy people and cancer patients. Laser desorption/ionization mass spectrometry on gold nanostructures-based techniques were used for the metabolic analysis of urine of 50 patients with kidney cancer. Comparison with data from 50 healthy volunteers led to the discovery of several compounds that may be considered potential renal cell carcinoma (RCC) biomarkers. Statistical analysis of data allowed for the discovery of *m*/*z* values that had the greatest impact on group differentiation. A database search enabled the assignment of signals for the most promising 15 features among them: serine, heptanol, 3-methylene-indolenine, 2-methyl-3-hydroxy-5-formylpyridine-4-carboxylate, phosphodimethylethanolamine, 4-methoxyphenylacetic acid, *N*-acetylglutamine, 3,5-dihydroxyphenylvaleric acid, hydroxyhexanoylglycine, valyl-leucine, leucyl-histidine, oleamide, 9,12,13-trihydroxyoctadecenoic acid, stearidonyl carnitine and squalene. Differences of metabolite profiles of human urine could be identified by gold nanoparticle-enhanced target (AuNPET) LDI MS method and used for the detection of renal cancer.

Keywords Cancer biomarker, gold nanoparticles, kidney cancer, laser desorption/ionization, mass spectrometry, renal cell carcinoma

(Received June 25, 2020; Accepted August 13, 2020; Advance Publication Released Online by J-STAGE August 21, 2020)

Introduction

Worldwide, every year brings 400000 new cases of kidney cancer and more than 175000 deaths due to this disease.[1] Renal cell carcinomas (RCCs)[2] are the sixth most frequently diagnosed cases of cancer in men and the tenth for women.[3,4] RCC can develop for a long time without clinical symptoms and a significant proportion of patients (25 – 30%) have metastases at the time of diagnosis.[5] For these reasons, it is important to develop new methods for early detection of RCC, among them the most important are based on specific chemical compounds, called biomarkers. Diagnostic biomarkers can be proteins,[6] genes[7] or metabolites.[8]

Due to the location of RCC inside the urine tract, urine is best suited for large-scale screening to detect diagnostic markers of renal cell carcinoma. Most kidney tumors occur in the tubular epithelium and cause the secretion of specific metabolites into their lumen. This process can be used to differentiate the urinary metabolome of sick and healthy people.[9] This approach has already been used several times by researchers who used various types of liquid chromatography combined with mass spectrometry.[10-14] Unfortunately, urine is characterized by high variability among patients depending on age, gender, diet and activity levels. Moreover, biomarkers usually are present in urine at very low concentrations.[15]

Commonly used for peptide and protein research, matrix-assisted laser desorption/ionization (MALDI) mass spectrometry has already been used for tumor marker research,[16,17] and also for RCC protein profiling.[18] However, MALDI spectra contain a high chemical background below *m*/*z* 1000 due to the use of organic matrices. For small molecules, surface-assisted laser desorption/ionization (SALDI)[19] solutions are generally better suited. A search of literature has shown, gold nanostructures are among the most frequently used for laser MS. Some of the recent applications of gold nanostructures in LDI MS include nanostructure-embedded micro gold shells previously applied for analysis of small molecules without any significant background interferences.[20] Colaianni *et al*. applied gold nanowires with good results for small peptide analysis.[21] Nanoflowers of Au@MnO were applied for analysis of small and also large molecules of cancer cell lysates.[22,23] Our group presented the advantages of gold-nanoparticle enhanced target (AuNPET) for laser desorption/ionization mass spectrometry analysis and imaging of low molecular weight compounds of different polarity, also in complex biological mixtures from plants,[24,25] human kidney tissue[26] and blood serum,[27] metabolome profiling of moulds,[28] as well as lysine amino acid detection and quantification.[29] Compared to commonly used MALDI MS,

† To whom correspondence should be addressed.
E-mail: adrian@arendowski.hub.pl

Table 1 Clinical characteristics of patients

		Patients
Total		50
Age/years		35 – 89
Mean		62
Sex	Male	30
	Female	20
Stage (T)	T1	33
	T2	3
	T3	10
	T4	1
Nodes (N)	Undefined	3
	N0	46
	N1	1
Metastases (M)	Undefined	3
	M0	42
	M1	5
Grade (Fuhrman)	Undefined	3
	I	7
	II	17
	III	13
	IV	2
	Undefined	11

the gold nanoparticle-based method has been proven to produce much lower chemical background, allows more precise internal calibration and is better suited for low and medium polar compounds.

The goal of this work is to demonstrate the capabilities of the AuNPET-LDI-MS method for rapid metabolic profiling of 50 urine samples of patients with diagnosed RCC and statistical comparison with a control group of 50 urine samples of healthy volunteers.

Experimental

Participants

Urine samples were obtained from 50 patients with diagnosed kidney cancer. The control was 50 urine samples from healthy volunteers, for which the presence of renal tumors had been excluded by abdominal ultrasound. Specimens and clinical data from patients involved in the study were collected with written consent. Patients who agreed to participate in the study donated 10 mL of blood and 50 mL of urine according to standard medical procedures. All experiments were performed in compliance with the local laws and institutional guidelines (Rzeszów University of Technology biological material guidelines). Research protocol was approved by the local bioethics committee at the University of Rzeszów (Poland). Patient characteristics are provided in Table 1.

The control group consisted of 50 healthy volunteers who donated 50 ml of urine. The average age was 50.6 years old and the male to female ratio was 3:2. Every volunteer underwent thorough abdominal ultrasound with the focus on the genitourinary system. No bladder or kidney tumors were diagnosed in this group.

Materials & methods

Chloro(trimethylphosphite)gold(I) of 97+% purity (Aldrich) was used for nanoparticle synthesis. The pyridine-borane complex (BH3:py) used had a borane concentration of ~8 M (Aldrich). All solvents were of HPLC quality and were purchased from Sigma-Aldrich (Poland), except for 18 MΩ water, which was produced locally. A magnetic stainless steel plate of H17 grade was made locally and used with a Bruker NALDI adapter.

Preparation of AuNPET target

Gold nanoparticle-enhanced target was prepared as described in our recent publication.[30] A stainless steel plate of 35 × 45 mm size was inserted into a large Petri dish containing acetonitrile (50 mL) and dissolved chloro(trimethylphosphite)gold(I) (25 mg). To this solution, 8 M BH3:py complex in pyridine (173 µL) was added. After 48 h of reaction, the target plate was washed several times with acetonitrile, wiped with cotton wool ball and washed three times with acetonitrile and deionized water.

Sample preparation

Urine samples obtained from patients were immediately frozen and stored at –60°C. Prior to measurements, an unfreezing step was performed in room temperature, followed by 1000-times dilution with ultrapure water. Volumes of 0.5 µL of urine solutions were placed directly on the target plate, air dried and inserted into the MS apparatus for measurements.

LDI MS experiment

Laser desorption/ionization mass spectrometry experiments were performed using a Bruker Autoflex Speed time-of-flight mass spectrometer equipped with a SmartBeam II laser (355 nm) in positive-ion reflectron mode. The measurement range was *m/z* 80 – 2000, suppression was turned on for *m/z* lower than 79. Laser impulse energy was approximately 100 – 190 µJ and laser repetition rate 1000 Hz. The number of laser shots was 20000 (4 × 5000 shots) for each sample spot. The first accelerating voltage was held at 19 kV and the second ion source voltage at 16.7 kV. Reflector voltages used were 21 kV (the first) and 9.55 kV (the second). The data was calibrated with FlexAnalysis (Ver. 3.3) using an enhanced cubic calibration model and analyzed with the mMass 5.5.0-open source program.[31] Mass calibration was performed using internal standards (gold ions and clusters from Au^+ to Au_5^+).

Analysis of MS results

A database search of chemical compounds was carried out using a custom made program. Theoretical *m/z* values were confirmed by using the ChemCalc program available online.[32] A statistical analysis of results was performed with the use of the MetaboAnalyst 4.0 service.[33] Data was normalized by sum, cube root transformed and default Pareto scaling was used. For creating receiver operating characteristic (ROC) curve, random forests has been chosen as a classification method and RandomForest built-in was selected as a feature ranking method.

Results and Discussion

In order to estimate the degree of influence of method-related spectral data over sample-related data, a statistical analysis with the aid of MetaboAnalyst 4.0 was performed. Principal component analysis (PCA), partial least squares-discriminant analysis (PLS-DA), sparse partial least squares-discriminant analysis (sPLS-DA) and orthogonal-orthogonal projections to latent structures-discriminant analysis (OPLS-DA) statistical methods implemented in MetaboAnalyst service were used. In case of domination of method-related data or signals, statistical analysis could not provide clear enough separation of studied samples.

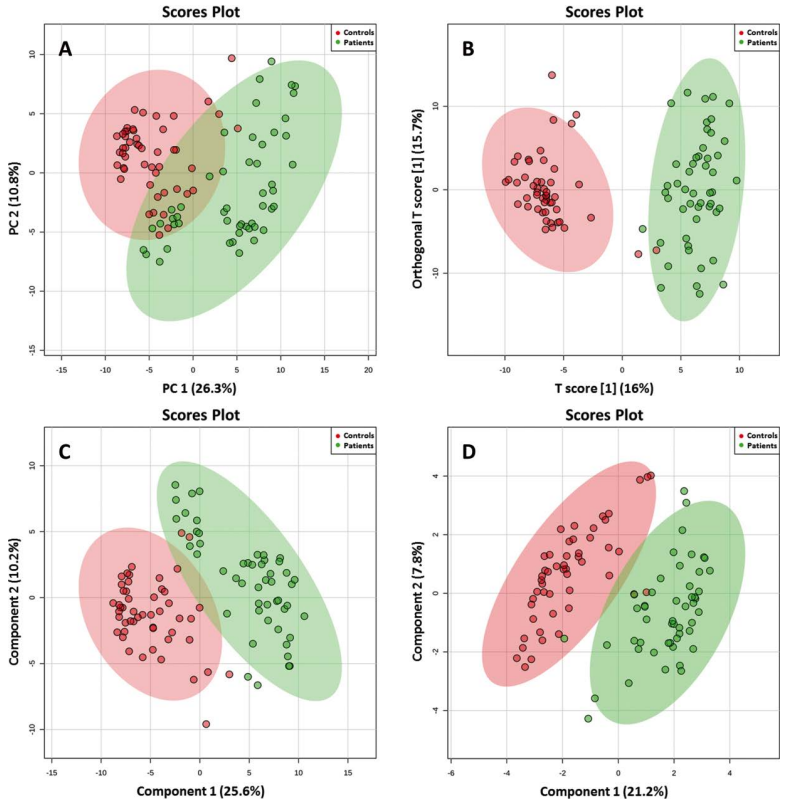

Fig. 1 Graphical representation of statistical analysis of MS data: PCA—component 1 *vs.* 2 (A), OPLS-DA (B), PLS-DA—component 1 *vs.* 2 (C), and sPLS-DA—component 1 *vs.* 2 (D). Red area represents data for controls while green for cancer patients.

Table 2 List of ions and compounds found by statistical analysis of mass spectra

Metabolite	Ion formula	Experimental *m/z*	Calculated *m/z*	Δ*m/z*, ppm	Reg.[a]	AUC	VIP[b]	*P*-Value[c]	Log 2 (FC)[d]	Fig.
Serine	$[C_3H_7NO_3 + K]^+$	144.0051	144.0058	–4.9	↓	0.561	1.22	3.9×10^{-11}	2.30	2A
Heptanol	$[C_7H_{16}O + K]^+$	155.0848	155.0833	9.7	↑	0.757	1.36	5.2×10^{-7}	–1.97	2B
3-Methylene-indolenine	$[C_9H_7N + K]^+$	168.0210	168.0210	0	↓	0.678	1.63	2.0×10^{-14}	4.70	2C
2-Methyl-3-hydroxy-5-formylpyridine-4-carboxylate	$[C_8H_7NO_4 + H]^+$	182.0445	182.0448	–1.6	↓	0.716	1.72	9.7×10^{-18}	3.78	2D
Phosphodimethylethanolamine	$[C_4H_{12}NO_4P + Na]^+$	192.0382	192.0396	–7.3	↓	0.579	1.15	8.5×10^{-10}	3.25	2E
4-Methoxyphenylacetic acid	$[C_9H_{10}O_3 + K]^+$	205.0280	205.0262	8.8	↓	0.600	1.16	7.5×10^{-9}	2.11	2F
N-Acetylglutamine	$[C_7H_{12}N_2O_4 + Na]^+$	211.0715	211.0689	12.3	↑	0.813	2.38	1.4×10^{-7}	–1.30	2G
3,5-Dihydroxyphenylvaleric acid	$[C_{11}H_{14}O_4 + H]^+$	211.0990	211.0965	11.8	↓	0.844	3.18	1.2×10^{-13}	9.66	2H
Hydroxyhexanoylglycine	$[C_8H_{15}NO_4 + Na]^+$	212.0891	212.0893	–0.9	↓	0.628	1.61	8.9×10^{-8}	1.32	3A
ValLeu	$[C_{11}H_{22}N_2O_3 + Na]^+$	253.1492	253.1523	–12.2	↓	0.706	1.60	4.1×10^{-10}	1.44	3B
LeuHis	$[C_{12}H_{20}N_4O_3 + H]^+$	269.1585	269.1608	–8.5	↑	0.661	1.34	3.0×10^{-7}	–4.14	3C
Oleamide	$[C_{18}H_{35}NO + Na]^+$	304.2630	304.2611	6.2	↑	0.599	1.24	1.7×10^{-2}	–1.74	3D
9,12,13-Trihydroxyoctadecenoic acid	$[C_{18}H_{34}O_5 + Na]^+$	353.2263	353.2298	–9.9	↑	0.741	1.88	4.1×10^{-3}	–1.44	3E
Stearidonyl carnitine	$[C_{25}H_{41}NO_4 + Na]^+$	442.2921	442.2928	–1.6	↑	0.658	0.96	7.4×10^{-3}	–1.41	3F
Squalene	$[C_{30}H_{50} + K]^+$	449.3511	449.3544	–7.3	↑	0.634	0.87	1.5×10^{-2}	–1.35	3G

a. Regulation of the intensity in RCC samples compared to control. b. VIP value obtained on the basis of PLS-DA analysis. c. *P*-Value obtained on the basis of the *t*-test statistical method. d. Value of log 2 of fold change between controls and cancer samples.

Figure 1 contains results of the statistical analysis of mass spectrometry data. It could be concluded that none of the used statistical methods: PCA (Fig. 1A), OPLS-DA score plot (Fig. 1B), PLS-DA (Fig. 1C) and sPLS-DA (Fig. 1D), not allowed for complete separation of cancer patients and the control group. These results are not unexpected as cancer and control samples are very similar from a molecular point of view, and complete separation in PCA is usually not visible. Moreover, the studied cancer group originates from patients with cancer of various stages and grades.

Based on PLS-DA, fold-change and random forest classification statistical methods, *m/z* values that had the greatest impact on group separation were obtained. Signals were assigned with the aid of Human Metabolome Database

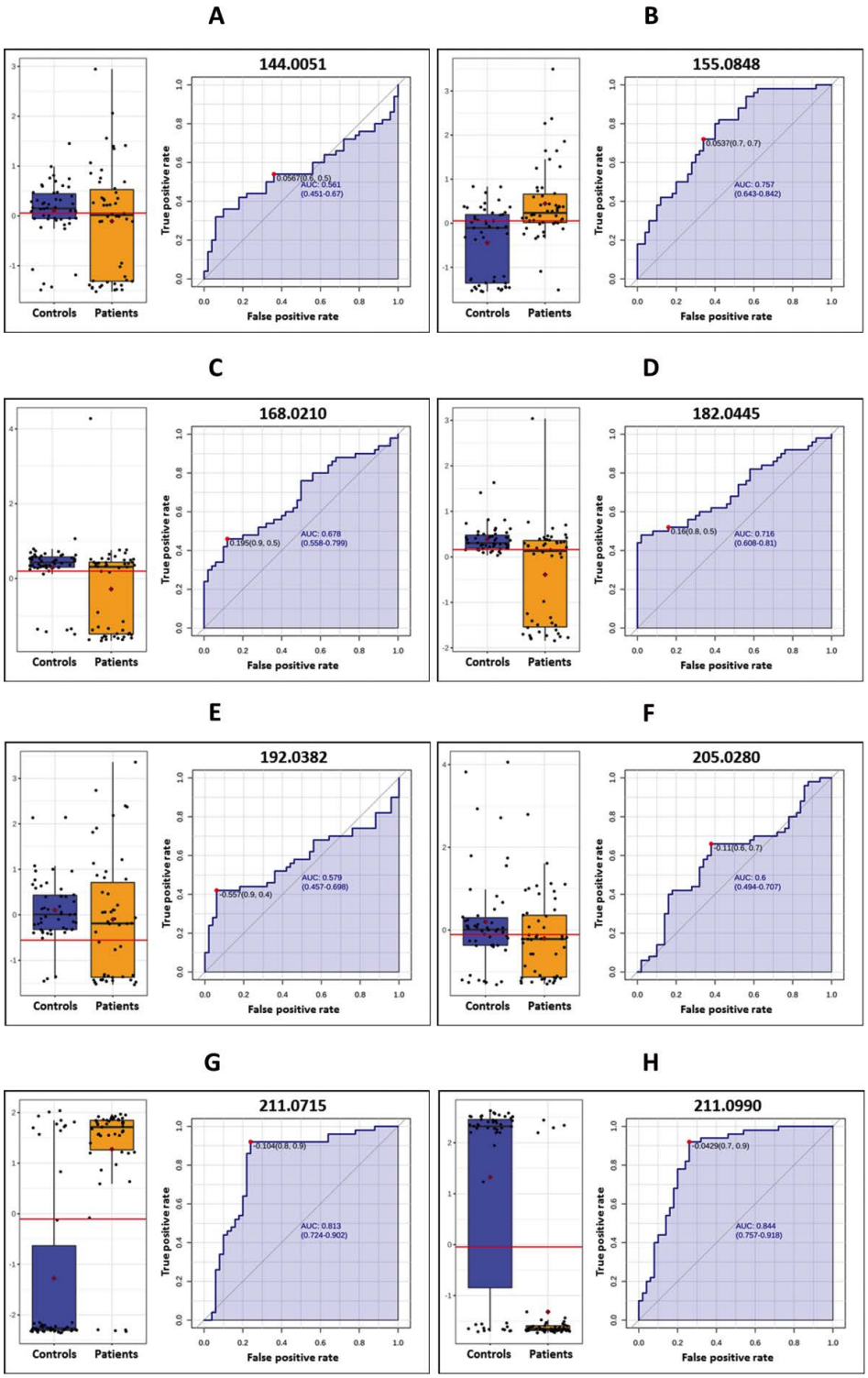

Fig. 2 Box plots and ROC curves for *m*/*z* values: 144.0051 (A), 155.0848 (B), 168.0210 (C), 182.0445 (D), 192.0382 (E), 205.0280 (F), 211.0715 (G) and 211.0990 (H).

(HMDB),[34] which allowed for the listing of 15 potential biomarkers shown in Table 2. The Random Forest classification method allowed the out-of-bag (OOB) error to be determined at the 0.04 level, correctly classifying healthy people to the control group in 94%, and people with diagnosed kidney cancer as patients in 98%, based on all signals present in mass spectra.

Figure 2 presents box plots and ROC curves for each of the 15 *m*/*z* values. The largest area under the curve (AUC) was recorded for *m*/*z* 211.0990 and is 0.844, while the smallest for *m*/*z* 144.0051 is 0.561. Seven of the proposed biomarkers show up-regulation in urine samples from patients with kidney cancer, others have higher intensities in the control samples. Fourteen of the metabolites shown in Table 2 have not previously been described as a potential RCC biomarker. Only squalene was previously proposed as a tissue biomarker of kidney cancer.[35] However, our results suggest higher intensities among urine of

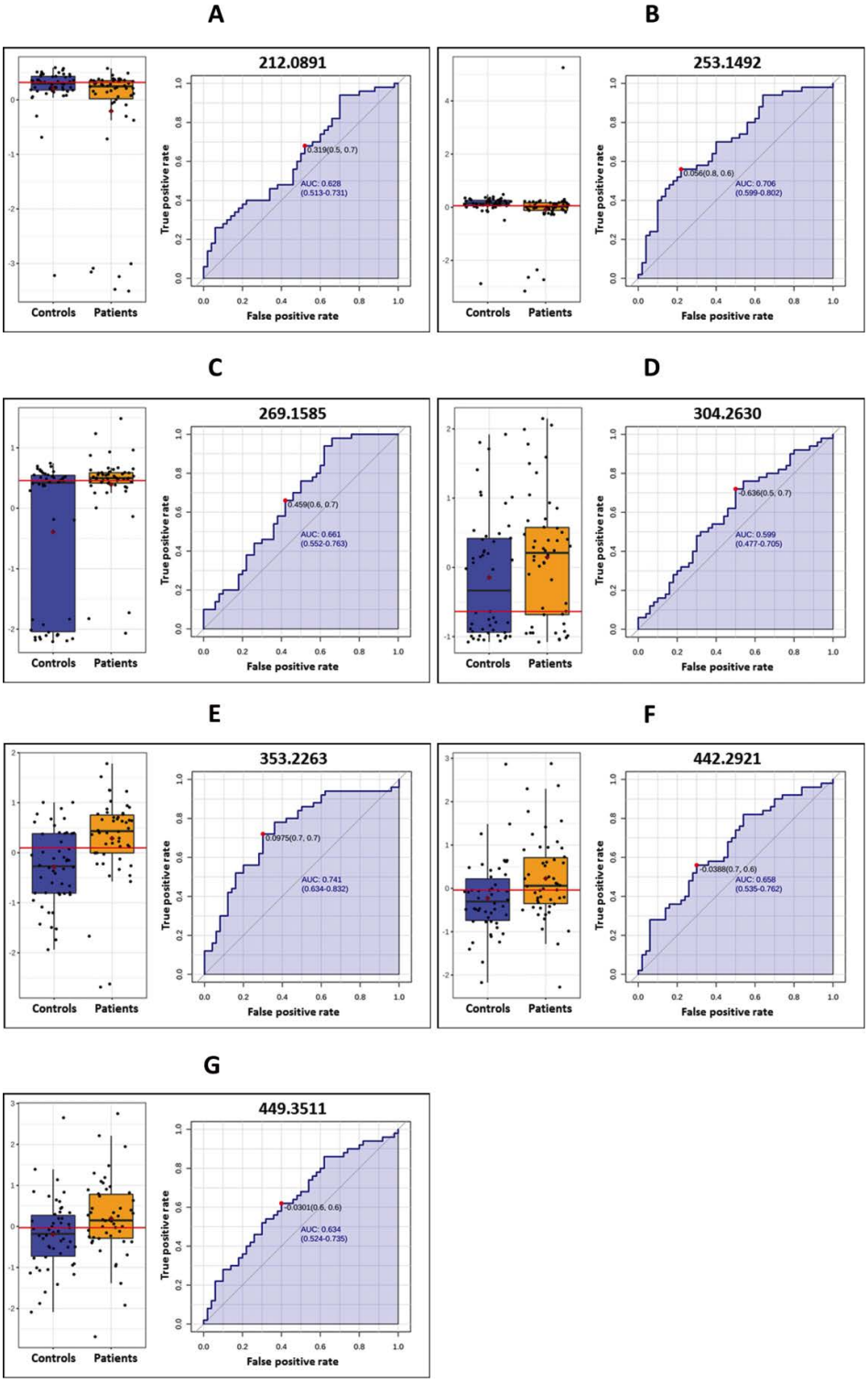

Fig. 3 Box plots and ROC curves for *m/z* values: 212.0891 (A), 253.1492 (B), 269.1585 (C), 304.2630 (D), 353.2263 (E), 442.2921 (F) and 449.3511 (G).

cancer patients (Fig. 3G). Squalene is polyunsaturated hydrocarbon occurring naturally in living organisms. It is a metabolic precursor of sterols, including cholesterol, steroid hormones and vitamin D. It has been shown that kidneys are one of the organs involved in the synthesis of squalene.[36] Moreover, it is believed that squalene molecules may play a role in inhibiting tumor growth.[37]

The first feature with higher mean intensity in cancer samples was *m/z* 155.0848 (Fig. 2B), which corresponds to the potassium cation adduct of $C_7H_{16}O$. A metabolite of this formula is heptanol, belonging to the class of organic compounds known as fatty alcohols. The next *m/z* value for which up-regulation was observed in cancer parients (Fig. 2G) was 211.0715, with one of the largest area under the curve of 0.813. This value has been assigned to sodium adduct of *N*-acetylglutamine, a derivative of amino acid. *N*-Acetylglutamine has already been

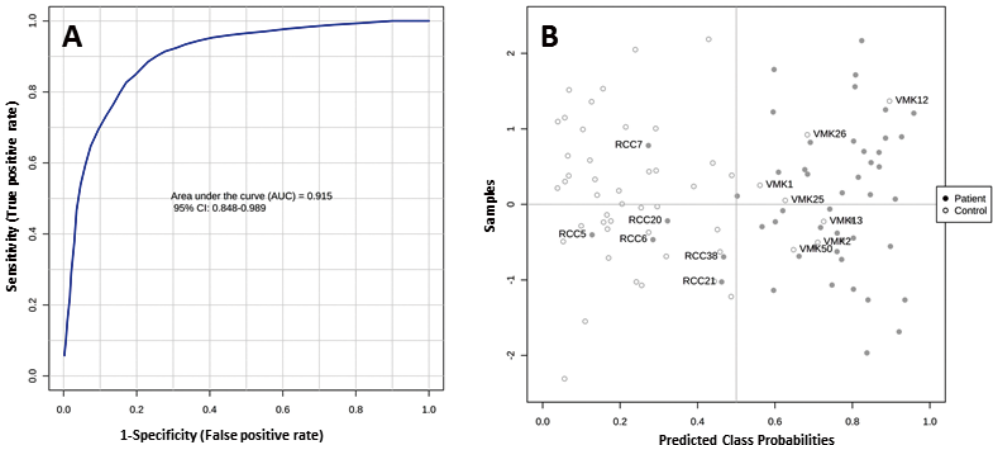

Fig. 4 Multivariate ROC curve based exploratory analysis based on 15-features intensity data processed using the MetaboAnalyst service, showing area under the curve (A) and predicted class probabilities for each sample with label samples classified to the wrong groups (B).

detected in human urine by LC-MS.[38] It was also found that increasing the concentration of this metabolite in urine may suggest renal tubular injury.[39] Another *m*/*z* value with higher intensities in cancer samples was 269.1585 (Fig. 3C) assigned to proton adduct of dipeptide LeuHis, a product of protein breakdown. The compound attributed to *m*/*z* 304.2630 is oleamide for which we observed up-regulation in urine of patients with renal cell carcinoma (Fig. 3D). Oleamide is an amide of oleic acid and it occurs naturally in the body as a sleep inducing lipid whose mechanism of action is still not well understood.[40] Studies suggest that this lipid may change its function in the urinary system, causing increased calcium in bladder cancer and renal cells.[41] Interestingly, the increase in oleamide levels was detected by chromatographic methods in the serum of people with colorectal cancer.[42]

9,12,13-Trihydroxyoctadecenoic acid is a molecule assigned to a *m*/*z* 353.2263 showing higher intensity in the urine of RCC patients compared to controls with AUC equal to 0.741 (Fig. 3E). This compound is metabolite of linoleic acid, and its increased concentration was detected in the blood of people with prostate cancer.[43] A feature with up-regulation in RCC samples is *m*/*z* 442.2921 attributed to sodium adduct of stearidonyl carnitine (Fig. 3F). Acylcarnitine to which this molecule belongs was previously found in higher concentrations than in the control group in the tissues and urine of patients with kidney cancer.[13,14]

For the remaining eight metabolites (serine, 3-methylene-indolenine, 2-methyl-3-hydroxy-5-formylpyridine-4-carboxylate, phosphodimethylethanolamine, 4-methoxyphenylacetic acid, 3,5-dihydroxyphenylvaleric acid, hydroxyhexanoylglycine and valyl-leucine), down-regulation was observed for cancer samples. Serine deserves special attention among these compounds. Serine biosynthesis also affects cellular antioxidative capacity, thus supporting tumor homeostasis and it has been shown that metabolic enzymes of serine biosynthesis are up-regulated in cancer.[44] However, a decrease in serum serine and urine and an increase in tissue are observed in human colorectal cancer,[42] which is consistent with our results for renal cell carcinoma.

For all 15 signals, an intensity table was created based on individual spectra from each sample and then receiver operating characteristic (ROC) analysis was performed in MetaboAnalyst 4.0. The results of the analysis are presented in Fig. 4. The area under the curve (AUC) for the proposed biomarkers was found to be 0.915 (Fig. 4A), thus they have high diagnostic accuracy to distinguish patients with kidney cancer from the healthy people in the control group. Predicted class probabilities for each sample shown in Fig. 4B were made on the basis of AUC. Cross-validation allowed for correct classification of 44 samples to be qualified as originating from patients with kidney cancer, which gives 88% efficiency and 43 samples as derived from healthy volunteers, giving 86% correctness.

Conclusions

Laser desorption/ionization mass spectrometry with gold nanoparticle-enhanced SALDI-type target was used for rapid analysis of urine from 50 patients with diagnosed kidney cancer and 50 healthy volunteers. The methodology allowed for the identification of 15 up- and down-regulated compounds that could potentially serve as renal cancer biomarkers. The 15 compounds are serine, heptanol, 3-methylene-indolenine, 2-methyl-3-hydroxy-5-formylpyridine-4-carboxylate, phospho-dimethylethanolamine, 4-methoxyphenylacetic acid, *N*-acetyl-glutamine, 3,5-dihydroxyphenylvaleric acid, hydroxyhexanoyl-glycine, valyl-leucine, leucyl-histidine, oleamide, 9,12,13-trihydroxyoctadecenoic acid, stearidonyl carnitine and squalene. Multivariate ROC analysis proposed biomarkers gave an area under the curve equal to 0.915, and correct classification of patients and healthy people at 87%. Statistical analysis allowed to distinguish the study group from the control.

Acknowledgements

This scientific work was funded by the Ministry of Science and Higher Education Republic of Poland from the budget for science in the years 2016 – 2020 as a research project within the program “Diamond Grant” (project no. 0184/DIA/2016/45). Mr Dominik Ruman is acknowledged for creating the MS search engine of chemical compounds.

References

1. F. Bray, J. Ferlay, I. Soerjomataram, R. L. Siegel, L. A.

Torre, and A. Jemal, *CA Cancer J. Clin.*, **2018**, *68*, 394.
2. W.-H. Chow, L. M. Dong, and S. S. Devesa, *Nat. Rev. Urol.*, **2010**, *7*, 245.
3. R. L. Siegel, K. D. Miller, and A. Jemal, *CA Cancer J. Clin.*, **2018**, *68*, 7.
4. U. Capitanio, K. Bensalah, A. Bex, S. A. Boorjian, F. Bray, J. Coleman, J. L. Gore, M. Sun, C. Wood, and P. Russo, *Eur. Urol.*, **2019**, *75*, 74.
5. K. Gupta, J. D. Miller, J. Z. Li, M. W. Russell, and C. Charbonneau, *Cancer Treat. Rev.*, **2008**, *34*, 193.
6. T. C. Ngo, C. G. Wood, and J. A. Karam, *Urol. Oncol. Semin. Orig. Investig.*, **2014**, *32*, 243.
7. B. N. Lasseigne, T. C. Burwell, M. A. Patil, D. M. Absher, J. D. Brooks, and R. M. Myers, *BMC Med.*, **2014**, *12*, 235.
8. M. S. Monteiro, M. Carvalho, M. de Lourdes Bastos, and P. G. de Pinho, *Metabolomics*, **2014**, *10*, 1210.
9. S. Ganti and R. H. Weiss, *Urol. Oncol. Semin. Orig. Investig.*, **2011**, *29*, 551.
10. T. Kind, V. Tolstikov, O. Fiehn, and R. H. Weiss, *Anal. Biochem.*, **2007**, *363*, 185.
11. K. Kim, P. Aronov, S. O. Zakharkin, D. Anderson, B. Perroud, I. M. Thompson, and R. H. Weiss, *Mol. Cell. Proteomics*, **2009**, *8*, 558.
12. K. Kim, S. L. Taylor, S. Ganti, L. Guo, M. V. Osier, and R. H. Weiss, *OMICS J. Integr. Biol.*, **2011**, *15*, 293.
13. S. Ganti, S. L. Taylor, K. Kim, C. L. Hoppel, L. Guo, J. Yang, C. Evans, and R. H. Weiss, *Int. J. Cancer*, **2012**, *130*, 2791.
14. J. Nizioł, V. Bonifay, K. Ossoliński, T. Ossoliński, A. Ossolińska, J. Sunner, I. Beech, A. Arendowski, and T. Ruman, *Anal. Bioanal. Chem.*, **2018**, *410*, 3859.
15. C. Bax, G. Taverna, L. Eusebio, S. Sironi, F. Grizzi, G. Guazzoni, and L. Capelli, *Cancers*, **2018**, *10*, 123.
16. H. Bateson, S. Saleem, P. M. Loadman, and C. W. Sutton, *J. Pharmacol. Toxicol. Methods*, **2011**, *64*, 197.
17. M. A. Merlos Rodrigo, O. Zitka, S. Krizkova, A. Moulick, V. Adam, and R. Kizek, *J. Pharm. Biomed. Anal.*, **2014**, *95*, 245.
18. E. Gianazza, C. Chinello, V. Mainini, M. Cazzaniga, V. Squeo, G. Albo, S. Signorini, S. S. Di Pierro, S. Ferrero, S. Nicolardi, Y. E. M. van der Burgt, A. M. Deelder, and F. Magni, *J. Proteomics*, **2012**, *76*, 125.
19. J. Sunner, E. Dratz, and Y.-C. Chen, *Anal. Chem.*, **1995**, *67*, 4335.
20. J. Lee, J. Lee, T. D. Chung, and W.-S. Yeo, *Anal. Chim. Acta*, **2012**, *736*, 1.
21. L. Colaianni, S. C. Kung, D. K. Taggart, R. A. Picca, J. Greaves, R. M. Penner, and N. Cioffi, *Anal. Bioanal. Chem.*, **2014**, *406*, 4571.
22. I. Ocsoy, B. Gulbakan, M. I. Shukoor, X. Xiong, T. Chen, D. H. Powell, and W. Tan, *ACS Nano*, **2013**, *7*, 417.
23. H. N. Abdelhamid and H.-F. Wu, *Anal. Bioanal. Chem.*, **2016**, *408*, 4485.
24. J. Sekuła, J. Nizioł, M. Misiorek, P. Dec, A. Wrona, A. Arendowski, and T. Ruman, *Anal. Chim. Acta*, **2015**, *895*, 45.
25. A. Arendowski and T. Ruman, *Phytochem. Anal.*, **2017**, *28*, 448.
26. J. Nizioń, K. Ossoliński, T. Ossoliński, A. Ossolińska, V. Bonifay, J. Sekuła, Z. Dobrowolski, J. Sunner, I. Beech, and T. Ruman, *Anal. Chem.*, **2016**, *88*, 7365.
27. A. Arendowski, K. Ossoliński, J. Nizioł, and T. Ruman, *Int. J. Mass Spectrom.*, **2020**, *456*, 116396.
28. A. Arendowski, J. Szulc, J. Nizioł, B. Gutarowska, and T. Ruman, *Anal. Biochem.*, **2018**, *549*, 45.
29. A. Arendowski and T. Ruman, *Anal. Methods*, **2018**, *10*, 5398.
30. J. Sekuła, J. Nizioł, W. Rode, and T. Ruman, *Anal. Chim. Acta*, **2015**, *875*, 61.
31. T. H. J. Niedermeyer and M. Strohalm, *PLoS ONE*, **2012**, *7*, e44913.
32. L. Patiny and A. Borel, *J. Chem. Inf. Model.*, **2013**, *53*, 1223.
33. J. Chong, D. S. Wishart, and J. Xia, *Curr. Protoc. Bioinforma.*, **2019**, *68*, e86.
34. D. S. Wishart, Y. D. Feunang, A. Marcu, A. C. Guo, K. Liang, R. Vázquez-Fresno, T. Sajed, D. Johnson, C. Li, N. Karu, Z. Sayeeda, E. Lo, N. Assempour, M. Berjanskii, S. Singhal, D. Arndt, Y. Liang, H. Badran, J. Grant, A. Serra-Cayuela, Y. Liu, R. Mandal, V. Neveu, A. Pon, C. Knox, M. Wilson, C. Manach, and A. Scalbert, *Nucleic Acids Res.*, **2018**, *46*, D608.
35. A. Arendowski, J. Nizioł, K. Ossoliński, A. Ossolińska, T. Ossoliński, Z. Dobrowolski, and T. Ruman, *Bioanalysis*, **2018**, *10*, 83.
36. J. Edmond, A. Fogelman, and G. Popjak, *Science*, **1976**, *193*, 154.
37. H. L. Newmark, *Ann. N. Y. Acad. Sci.*, **1999**, *889*, 193.
38. K. Sugahara, J. Zhang, and H. Kodama, *J. Chromatogr. B Biomed. Appl.*, **1994**, *657*, 15.
39. S. X. Racine, P. Le Toumelin, F. Adnet, Y. Cohen, M. Cupa, E. Hantz, and L. Le Moyec, *Nephron Physiol.*, **2004**, *97*, 53.
40. D. Lambert and V. Di Marzo, *Curr. Med. Chem.*, **1999**, *6*, 757.
41. Y.-K. Lo, K.-Y. Tang, W.-N. Chang, C.-H. Lu, J.-S. Cheng, K.-C. Lee, K.-J. Chou, C.-P. Liu, W.-C. Chen, W. Su, Y.-P. Law, and C.-R. Jan, *Biochem. Pharmacol.*, **2001**, *62*, 1363.
42. Y. Ni, G. Xie, and W. Jia, *J. Proteome Res.*, **2014**, *13*, 3857.
43. R. M. Maxim, C. Socaciu, A. D. Buzoianu, R. M. Pop, and F. Romanciuc, *Bull. Univ. Agric. Sci. Vet. Med. Cluj-Napoca Food Sci. Technol.*, **2014**, *71*, 165.
44. I. Amelio, F. Cutruzzolá, A. Antonov, M. Agostini, and G. Melino, *Trends Biochem. Sci.*, **2014**, *39*, 191.